NANO LETTERS

2006
Vol. 6, No. 12
2868−2872

# Melt Coaxial Electrospinning: A Versatile Method for the Encapsulation of Solid Materials and Fabrication of Phase Change Nanofibers

**Jesse T. McCann,[†] Manuel Marquez,[‡] and Younan Xia*[,†]**

*Department of Chemistry, University of Washington, Seattle, Washington 98195-1700, and The INEST Group, Research Center, Philip Morris USA, Richmond, Virginia 23234*

*Received September 5, 2006; Revised Manuscript Received October 18, 2006*

**ABSTRACT**

**We have developed a method based on melt coaxial electrospinning for fabricating phase change nanofibers consisting of long-chain hydrocarbon cores and composite sheaths. This method combines melt electrospinning with a coaxial spinneret and allows for nonpolar solids such as paraffins to be electrospun and encapsulated in one step. Shape-stabilized, phase change nanofibers have many potential applications as they are able to absorb, hold, and release large amounts of thermal energy over a certain temperature range by taking advantage of the large heat of fusion of long-chain hydrocarbons. We have focused on compounds with melting points near room temperature (octadecane) and body temperature (eicosane) as these temperature ranges are most valuable in practice. We have produced thermally stable, phase change materials up to 45 wt % octadecane, as measured by differential scanning calorimetry. In addition, the resultant fibers display novel segmented morphologies for the cores due to the rapid solidification of the hydrocarbons driven by evaporative cooling of the carrier solution. Aside from the fabrication of phase change nanofibers, the melt coaxial method is promising for applications related to microencapsulation and controlled release of drugs.**

The encapsulation of an active substance in a matrix on the nanoscale is currently of great interest as it allows for the stabilization and tuning of the properties of the active material. To this end, encapsulation has been exploited for controlled release, as well as stabilization and immobilization of catalysts.[1] Recently, encapsulation has also found use in the production of phase change materials (PCMs)—materials that have melting points near the temperature of interest such that their heats of fusion can buffer temperature variation in the environment.[2] These materials can absorb, retain, and release large amounts of thermal energy as they go through phase transitions at their melting points. This allows for the storage of energy and also gives the insulating material a new function—stabilization of temperature. Due to the increase in energy prices and the demand for high-performance materials for thermal energy management, PCMs have lately become a subject of active research in both industry and academia.[3]

Because PCMs melt and crystallize repeatedly during use, it is necessary to stabilize them in a solid matrix. Various inorganic and organic materials have been examined for their potential as PCMs.[4] For instance, hydrated salts have been investigated by a number of groups for solar energy storage applications.[5] Hydrocarbons such as paraffins have also been of interest, as they display extensive thermal stability and are less corrosive than the inorganic compounds studied.[6] Hydrocarbon PCMs have been incorporated into matrices such as shape-stabilized paraffins[7] and unsaturated polyester.[8] They have also been encapsulated in micrometer-sized particles. For example, Cho and co-workers have reported the encapsulation of octadecane in polyurea shells by interfacial polymerization.[9] Using this method, octadecane@polyurea microspheres containing 26−46% octadecane by weight have been successfully prepared. For most applications, these core−shell particles would then need to be incorporated into fibers, thus decreasing the weight percent of encapsulated octadecane. In general, direct encapsulation of PCMs in a fibrous matrix should allow for greater insulating capacity. Fibrous matrices are also immediately useful as high-performance nonwoven fabrics and coatings.[10]

Here we combine melt electrospinning with coaxial spinneret to provide a facile method for the encapsulation of solids in a composite or polymer matrix to generate nanofiber-based PCMs. Electrospinning relies on the use of

* To whom correspondence should be addressed. E-mail: xia@chem.washington.edu
[†] Department of Chemistry, University of Washington.
[‡] The INEST Group, Research Center, Philip Morris USA.

10.1021/nl0620839 CCC: $33.50 
**Published on Web 11/04/2006**

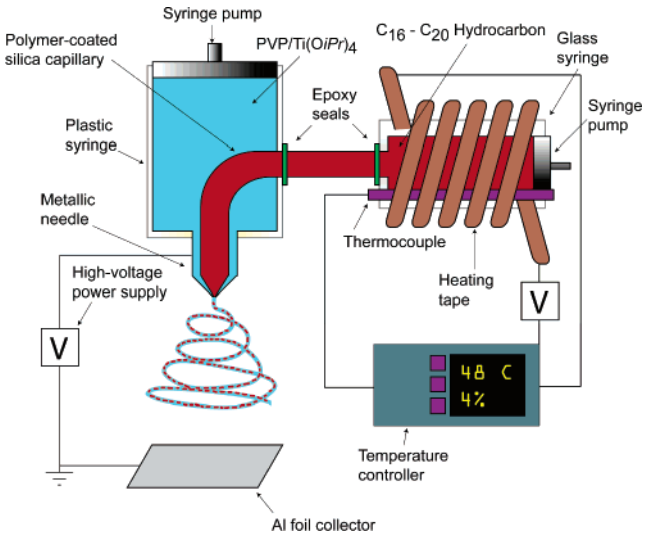


**Figure 1.** Schematic of the melt coaxial electrospinning setup used for fabricating $TiO_2$−PVP nanofibers loaded with hydrocarbon PCMs.

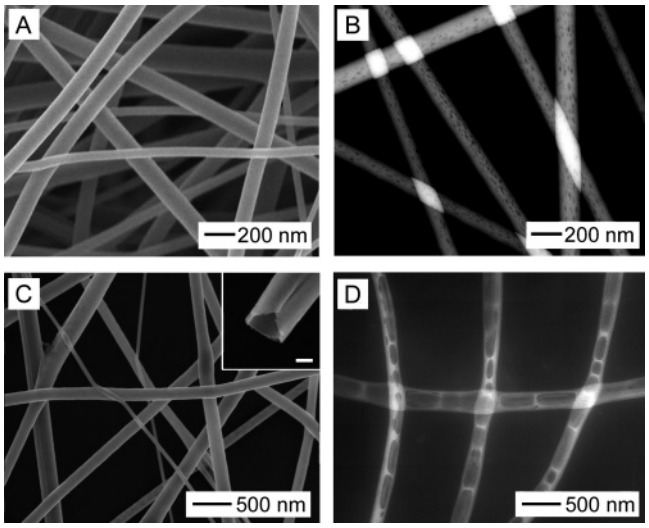


**Figure 2.** Octadecane@$TiO_2$−PVP nanofibers electrospun with a melt coaxial spinneret. (A) SEM image of the nanofibers with 7% octadecane loading as determined by DSC. (B) TEM image of the fibers with the octadecane having been removed by soaking in hexane for 24 h. (C) SEM image of octadecane@$TiO_2$−PVP nanofibers with 45% octadecane loading as determined by DSC. (D) TEM image of these fibers after the octadecane had been removed by soaking in hexane for 24 h. The scale bar in the inset of panel C is 100 nm.

a high-voltage electric field to draw a viscous droplet into an elongated jet.[11] A dynamic instability results in whipping and stretching which is responsible for the attenuation of the jet into long fibers with ultrathin diameters. Electrospinning is remarkably simple and versatile and capable of producing nano- and microscale fibers in large quantities. Polymer solutions are predominantly used in this process, though composites, sol−gels, and surfactant-based solutions have also been included to fabricate nanofibers with a broad range of compositions, morphologies, and properties.[12]

Melt coaxial electrospinning provides a simple method for the encapsulation of solid materials and extends the technique to create new morphologies and architectures. Processing of fibers from melts is a widely used method in commercial fiber fabrication. Techniques such as melt spinning and melt blowing have already been used to fabricate nonwoven polymer fibers with diameters down to the nanoscale.[13] Melt electrospinning has several distinct advantages over its solution-based counterpart, most notably environmental friendliness and low cost due to the absence of solvent.[14] Using the melt electrospinning technique, commodity polymers such as poly(propylene) and poly(ethylene terephthalate) have been directly drawn into nonwoven fibers. The coaxial electrospinning technique has recently been developed by us and others to fabricate core−sheath and hollow nanofibers made of ceramics or composites.[15] By combining melt electrospinning and coaxial electrospinning, now we come up with a versatile route to the facile encapsulation of solid materials in nanofibers.

Figure 1 shows a schematic of the melt coaxial electrospinning setup. In our method, a coaxial spinneret is constructed by inserting a polymer-coated silica capillary into a plastic syringe and then concentrically into a metallic needle. This silica capillary is connected to a glass syringe that is placed in an insulated heating mantle. The temperature of the glass syringe is controlled by a temperature controller. With this spinneret, materials that are solid at room temperature can be injected concentrically into a spinning jet together with a carrier solution. During the spinning process, cooling of the jet due to solvent evaporation causes the inner liquid to quickly solidify, leading to its encapsulation in the nanofibers. Like conventional coaxial electrospinning, the inner material (in both melt and solid states) must be insoluble in the solvent used for the outer jet in order to obtain fibers with a core−sheath structure.

Figure 2 shows nanofibers that were fabricated using the melt coaxial spinneret. The sheath consisted of a $TiO_2$−PVP composite while the core was octadecane. The core material was heated to a temperature of 68 °C prior to injection and was fed at a rate of 0.2 mL/h while the sheath solution was fed at 0.7 mL/h. Figure 2A shows a scanning electron microscopy (SEM) image of the as-prepared fibers and Figure 2B shows the corresponding transmission electron microscopy (TEM) image of the fibers after they have been soaked in hexane for 24 h to remove the hydrocarbon core. These fibers were ∼150 nm in diameter and were free of beads. TEM reveals that the octadecane broke up into spherical droplets in the interior of each nanofiber. Differential scanning calorimetry (DSC) indicates that these fibers contained 7% octadecane by weight. Figure 2C shows fibers fabricated with a higher feeding rate for octadecane: the core and sheath solution was fed at a rate of 0.3 and 0.7 mL/h, respectively. These fibers contained 45% octadecane by weight as shown by DSC. The TEM image in Figure 2D indicates that the octadecane formed elongated, compartmentalized domains along the long axis of the fiber. The behavior of octadecane in the cores of these fibers is quite different from the behavior of mineral oil.[15d] This is due to the difference in their viscosity profiles. Heavy mineral oil has a relatively high and even viscosity, ranging from 85 to 66 cP between 10 and 40 °C, while octadecane has a

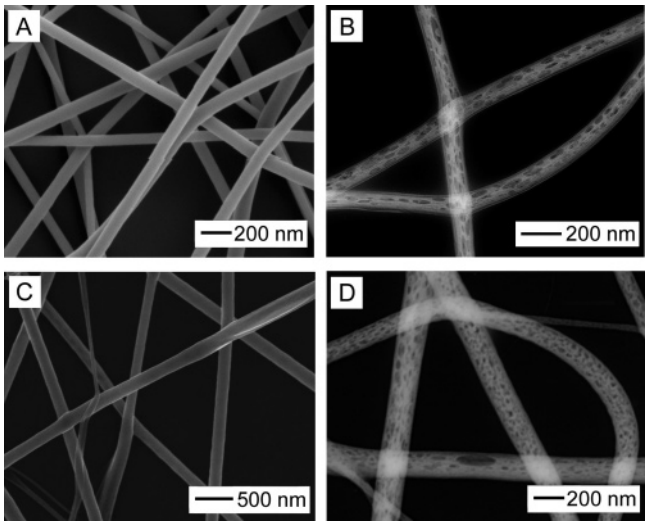


**Figure 3.** Demonstration of the versatility of the melt coaxial electrospinning technique. (A) SEM image of hexadecane@$TiO_2$−PVP fibers prepared using the melt coaxial electrospinning technique. (B) TEM image of these fibers with the hexadecane having been removed by soaking in hexane for 24 h. (C) SEM image of eicosane@$TiO_2$−PVP nanofibers fabricated using the melt coaxial electrospinning technique. (D) TEM image of these fibers after the eicosane was removed by a 24 h soak in hexane.

relatively low viscosity of 1.75 cP at 70 °C and 3.8 cP at 30 °C, and it crystallizes at 27 °C. The presence of droplets and segments inside the nanofibers indicates that varicose breakup of the octadecane occurred inside the spinning jet. The viscosity of the octadecane was too low to avoid varicose breakup, thus leading to the sprayed and/or segmented morphology. At low feeding rates, varicose breakup led to the dispersion of small droplets of octadecane throughout the nanofiber matrix. These droplets are stretched along the long axis of the fiber, as is consistent with electrohydrodynamic stretching of a nonconducting fluid. At high feeding rates, we also observed larger droplets of octadecane in the fibers, which were formed due to varicose breakup.

The melt coaxial electrospinning technique is versatile in that it can be used to incorporate materials with different melting points needed for phase change applications. Figure 3A shows SEM of fibers that incorporate hexadecane (mp = 16−17 °C) in $TiO_2$−PVP nanofibers. The fibers had a mean diameter of ∼100 nm. DSC measurement indicates that these nanofibers contained 31% hexadecane by weight. The corresponding TEM in Figure 3B shows that the hexadecane behaved analogously to octadecane in its breakup into small droplets, with their length stretched along the long axis of the fiber. Figure 3C shows SEM image of $TiO_2$−PVP fibers loaded with eicosane (mp = 35−37 °C). DSC reveals that these fibers contained 36% eicosane by weight. Since the melting point of eicosane is close to human body temperature, this material is ideal for phase change applications that involve high-performance fabrics.

Figure 4 shows Lissajous figures[16] constructed from DSC measurements on the phase change nanofibers fabricated by melt coaxial electrospinning. Figure 4A shows the thermal behavior of hexadecane@$TiO_2$−PVP nanofibers when cycled between 0 and 25 °C at 4 °C/min for five cycles, demonstrating a melting point of 16 °C and a freezing point of 11 °C. The enthalpy of melting by weight of the sample was measured to be 71 J/g, corresponding to 31% (by weight) loading of hexadecane. Figure 4B shows the behavior of octadecane@$TiO_2$−PVP nanofibers fabricated by melt coaxial electrospinning. The melting point of the octadecane in this preparation was found to be 27 °C, and the freezing point was found to be 19 °C by DSC measurement. The enthalpy of melting was found to be 114 J/g, corresponding to a loading of 45% octadecane by weight. Figure 4C shows the DSC measurement of eicosane@$TiO_2$−PVP nanofibers. The melting point of eicosane was found to be 37 °C, with an enthalpy of melting of 88 J/g, corresponding to 36% loading of eicosane by weight. Thermogravimetric analysis (TGA) of the samples held at 100 °C for 4 h shows no substantial mass change. These results clearly demonstrate that all the hydrocarbons have been successfully encapsulated

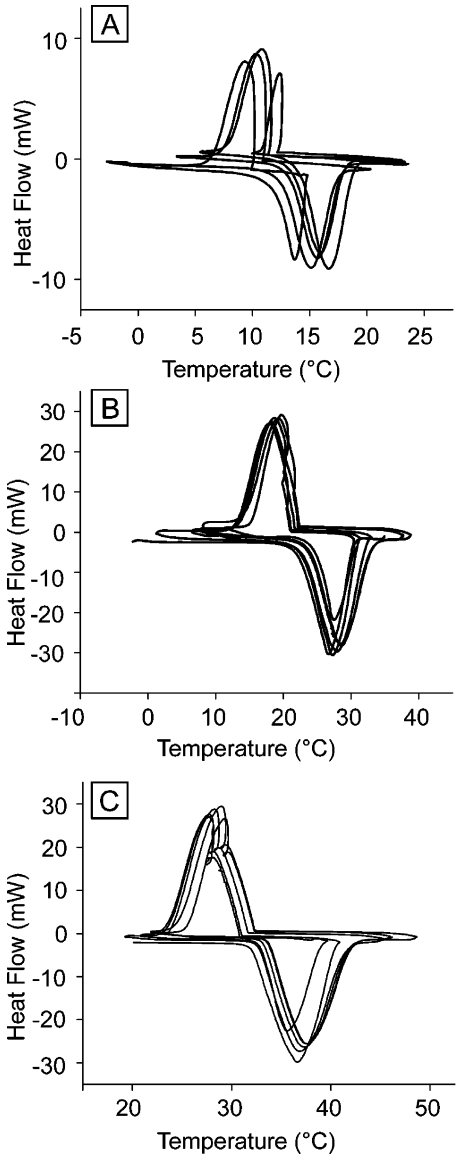


**Figure 4.** Lissajous figures derived from DSC measurements on nonwoven mates of PCM nanofibers with different compositions: (A) hexadecane@$TiO_2$−PVP; (B) octadecane@$TiO_2$−PVP; and (C) eicosane@$TiO_2$−PVP.

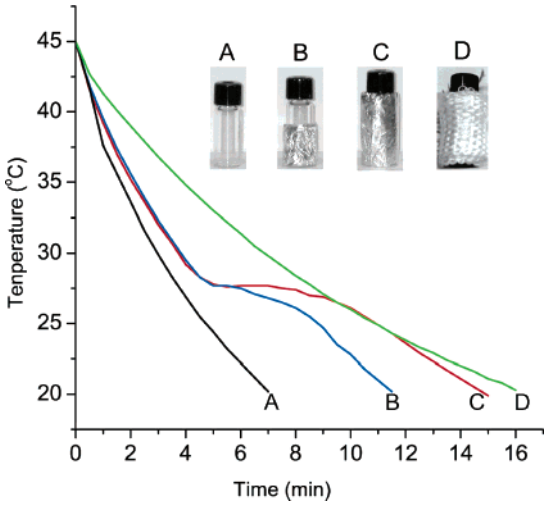


**Figure 5.** Demonstration of thermal insulation capability of octadecane@$TiO_2$−PVP nanofibers, where 1 $cm^3$ of water at 60 °C was allowed to cool in a 4 °C environment in glass vials covered with different insulation jackets. Sample A had no insulation, sample B was half covered with the PCM nanofiber jacket, and sample C was fully covered by the PCM nanofiber jacket. Sample D is covered by a jacket of conventional fiberglass.

in the nanofibers, as there was essentially no thermal evaporation in the heating process.

Figure 5 demonstrates the capability of these PCM nanofibers to stabilize temperature.[17] In this experiment, a borosilicate glass vial was covered with a different insulation jacket, filled with 1 $cm^3$ of 60 °C water and then allowed to cool in a 4 °C environment. The water temperature in the vial was measured using a thermal couple every 30 s and recorded until it reached 20 °C. Figure 5A shows a control where there was no insulation jacket on the glass vial. Figure 5B shows a sample half-insulated with a 2 mm thick layer of octadecane@$TiO_2$−PVP fibers sandwiched between Al foils. Figure 5C shows a sample in which the entire glass vial was insulated with the same jacket as in Figure 5B. Figure 5D shows a sample covered with an 8 mm thick jacket of fiberglass fibers. Supercooling was not observed in the temperature history curve for the PCM nanofibers. In addition, it is evident that the insulating capacity was reduced by the removal of PCM insulation, with the sample reaching 20 °C after 7 min for the uninsulated sample, 12 min for the sample with half-insulation, and 16 min for the sample that was fully covered by the PCM fibers. The fiberglass fibers were as effective as the PCM nanofibers in insulating the vial although the former jacket was approximately 4 times thicker than the PCM fiber-based one. More importantly, the jacket based on PCM fibers allowed one to stabilize the temperature (close to the melting point of octadecane) in the vial for 5 min. In contrast, the temperature continuously dropped with time for all other types of insulating jackets.

The melt coaxial electrospinning method is quite useful for the encapsulation of active solids in fibrous matrices. By combination of melt with coaxial spinneret, PCM nanofibers have been successfully fabricated. The development of this technique allows for the fabrication of fibers with new morphologies, as it relies on both evaporative solidification of the sheath solution and solidification of the core by freezing. Aside from encapsulating phase change solids, this method is extensible to functional solids with melting points between 10 and 80 °C. The fabrication of fibrous scaffolds for biomedical applications often relies on the stabilization and controlled release of small molecules; thus this method could also prove useful in this field.[18] In addition, small organics can be stabilized in paraffin droplets and then incorporated into a fibrous matrix, further enhancing the utility of melt coaxial electrospinning in industry. Further development of this technique will focus on the exploration of its potential for the fabrication of multifunctional nanofibers and assemblies.

**Experimental Section. Coaxial Electrospinning Setup.** To construct the melt coaxial electrospinning setup, a 100 $\mu$m diameter polyimide-coated silica capillary (Polymicro, Phoenix, AZ) was inserted concentrically into a metallic needle attached to a 3-mL plastic syringe (Becton Dickenson, Franklin Lakes, NJ) and fixed with epoxy (Devcon, Danvers, MA). To create a well for the molten hydrocarbons, a 2-mL glass syringe (Hamilton, Reno, NV) was wrapped with heating tape (VWR Scientific, Ventura, CA) attached to a thermocouple and temperature controller (Ace Glass, Vineland, NJ). The assembly was then covered by glass wool and controlled with a separate syringe pump. This well was then attached to the polyimide-coated silica capillary from the coaxial spinneret so that the solutions could be fed independently.

**Electrospinning.** In a typical procedure for melt coaxial electrospinning, a solution consisting of 0.3 g of PVP (Aldrich, $M_w \approx 1\,300\,000$), 3 g of titanium tetraisopropoxide (Aldrich), 2 mL of acetic acid, and 5 mL of ethanol was added to the outer carrier solution. For the fibers containing octadecane (ACROS Organics), the heating mantle was set at 68 °C, and the solutions were fed independently by syringe pumps (KDS-200, Stoelting, Wood Dale, IL). The feed rates were tuned for the desired loading of PCM. For the spinning of octadecane@$TiO_2$−PVP fibers, the temperature of the inner solution was held at 62 °C prior to injection. Samples were collected onto Si wafers (Silicon Sense, Nashua, NH) for SEM, onto carbon-coated Cu grids for TEM (Ted Pella, Redding, CA), and directly onto Al foils for thermal analysis.

**Characterization.** Samples were sputtered for 30 s with gold prior to SEM (FEI Sirion, Portland, OR). For TEM (JEOL JEM 1200EX), the samples were soaked for 24 h in hexane to remove the hydrocarbon cores prior to analysis. DSC (Shimadzu DSC-60) and TGA (Shimadzu TGA-50) were performed on 1−3 mg samples in Al pans. For differential scanning calorimetry, a 4 °C/min scanning rate was used. Thermal analysis was conducted using the Shimadzu TA-60 software.

**Acknowledgment.** This work was supported in part by an AFOSR-MURI grant on smart-skin materials awarded to the UW and a research fellowship from the David and Lucile Packard Foundation. Y.X. is a Camille Dreyfus Teacher Scholar (2002−2007). J.M. is partially supported by an INEST research fellowship. Part of the work was performed

at the Nanotech User Facility, a member of the National Nanotechnology Infrastructure Network (NNIN) funded by the NSF.

## References

(1) (a) Wilcox, D. L.; Berg, M.; Bernat, T.; Kellerman, D.; Cochran, J. K., Jr. *Mater. Res. Soc. Symp. Proc.* **1994**, *372*, 1−13. (b) Langer, R. *Nature* (suppl.) **1998**, *392*, 5. (c) Kawahashi, N.; Matijevič, E. *J. Colloid Interface Sci.* **1990**, *138*, 534. (d) Fleming, M. S.; Mandal, T. K.; Walt, D. R. *Chem. Mater.* **2001**, *13*, 2210. (e) Cohen, I.; Li, H.; Houghland, L.; Mrkisch, M.; Nagel, S. R. *Science* **2001**, *292*, 265.

(2) Zalba, B.; Marín, J. M.; Cabeza, L. F.; Mehling, H. *Appl. Thermal Eng.* **2003**, *23*, 251.

(3) Mulligan, J. C.; Colvin, D. P.; Bryant, Y. G. *J. Spacecr. Rockets* **1996**, *33*, 278.

(4) Brown, R. C.; Rasberry, J. D.; Overmann, S. P. *Powder Technol.* **1998**, *3*, 217.

(5) Li, J. H.; Zhang, G. E.; Wang, J. Y. *Sol. Energy* **1991**, *6*, 443.

(6) Himran, S; Suwono, A.; Mansoori, G. A. *Energy Sources* **1994**, *16*, 117.

(7) (a) Lee, C. H.; Choi, H. K. *Polym. Compos.* **1998**, *19*, 704. (b) Sari, A. *Energy Convers. Manage.* **2004**, *45*, 2033.

(8) Abhat, A. *Solar Energy* **1983**, *30*, 313.

(9) Cho, J. S.; Kwon, A.; Cho, C.-G. *Colloid Polym. Sci.* **2002**, *3*, 260.

(10) Ma, M.; Mao, Y.; Gupta, M.; Gleason, K. K.; Rutledge, G. C. *Macromolecules* **2005**, *38*, 9742.

(11) See recent reviews, (a) Reneker, D. H.; Chun, I. *Nanotechnology* **1996**, *7*, 216. (b) Li, D.; Xia, Y. *Adv. Mater.* **2004**, *16*, 1151.

(12) (a) Formhals, A. U.S. Patent 1,975,504, **1934**. (b) Doshi, J.; Reneker, D. H. *J. Electrost.* **1995**, *35*, 151. (c) Reneker, D. H.; Chun, I. *Nanotechnology* **1996**, *7*, 216. (d) Theron, A.; Zussman, E.; Yarin, A. L. *Nanotechnology* **2001**, *12*, 384. (e) McCann, J. T.; Chen, J.; Li, D.; Ye, Z.-G.; Xia, Y. *Chem. Phys. Lett.* **2006**, *424*, 162. (f) Jang, S.-Y.; Seshadri, V.; Khil, M.-S.; Kumar, A.; Marquez, M.; Mather, P.; Sotzing, G. A. *Adv. Mater.* **2005**, *17*, 2177. (g) Yu, J. H.; Fridrikh, S. V.; Rutledge, G. C. *Adv. Mater.* **2004**, *16*, 1562. (h) McCann, J. T.; Marquez, M.; Xia, Y. *J. Am. Ceram. Soc.* **2006**, *89*, 1861.

(13) Moore, E. S.; Papavassiliou, D; Shambaugh, R. L. *Int. Nonwovens J.* **2004**, *3*, 43.

(14) Lyons, J.; Li, C.; Ko, F. *Polymer* **2004**, *22*, 7597.

(15) (a) Li, D.; McCann, J. T.; Xia, Y. *Small* **2005**, *1*, 83. (b) Loscertales, I. G.; Barrero, A.; Marquez, M.; Spretz, R.; Velarde-Ortiz, R.; Larsen, G. *J. Am. Chem. Soc.* **2004**, *126*, 5376. (c) Li, D.; Babel, A.; Jenekhe, S.; Xia, Y. *Adv. Mater.* **2004**, *16*, 2062. (d) Li, D.; Xia, Y. *Nano Lett.* **2004**, *4*, 933. (e) McCann, J. T.; Li, D.; Xia, Y. *J. Mater. Chem.* **2005**, *15*, 735. (f) Sun, Z.; Zussman, E.; Yarin, A. L.; Wendorff, J. H.; Greiner, A. *Adv. Mater.* **2004**, *22*, 1929.

(16) Ishikiriyama, K.; Boller, A.; Wunderlich, B. *J. Therm. Anal.* **1997**, *50*, 547.

(17) Yinping, Z.; Yi, J.; Yi, J. *Meas. Sci. Technol.* **1999**, *10*, 201.

(18) Hollister, S. J. *Nat. Mater.* **2005**, *4*, 518.

NL0620839